OPEN ACCESS

1st International Electronic Conference on Materials
26 May - 10 June 2014

http://sciforum.net/conference/ecm-1

Article

Rhodium Adsorption on Valonea Resol Polymer

Mustafa Can [1,*]

[1] Sakarya University, Vocational School of Arifiye, 54580, Turkey; E-Mails: mstfacan@gmail.com

***** Author to whom correspondence should be addressed; E-Mail: mstfacan@gmail.com; Tel.: +9-0264 295 33 52; Fax: +9-0264 295 72 02.

Received: 3 April 2014 / Accepted: 8 April 2014 / Published: 26 May 2014

Abstract: A new adsorbent resin has been developed by immobilizing tannin acid with formaldehyde, and its adsorption properties to Rh^{3+} were investigated. Linear and nonlinear regression procedures have been applied to the Langmuir, Freundlich, Tempkin, Dubinin–Radushkevich, and Redlich-Peterson isotherms The resin exhibited good adsorption capacity towards Rh^{3+} from acidic aqueous solutions ($[H^+]$ = 1 M, $[Cl^-]$ = 10^{-3} M), which the equilibrium adsorption capacity was high up to 96,69 mg g^{-1} at 293 K. The adsorption isotherms could be well described by Langmiur equation. The experimental studies suggested that tannin formaldehyde resin was effective for the adsorption of Rh^{3+} from chloride acid solutions, and the loaded Rh^{3+} could be easily desorbed by 1 M HNO_3 + 0,1 M $NaClO_3$ solution mixture with hundred percent efficiency. Thermodynamic parameters such as the entropy change, enthalpy change and Gibb's free energy change were calculated. The adsorption of Rh^{3+} was an endothermic adsorption process. This suggested that the resin can be used as an active biosorbent for the recovery of Rh^{3+} from 1 M concentrated acidic solution.

Keywords: rhodium; tannin; polymer; resin; adsorption; resol; nonlinear regression

---

1. Introduction

Because of lower ore reserve and many different industrial applications, Platinum Group Metals (PGM) must be recycled. Adsorption of rhodium (III) from chlorine and other ligand containing aqueous solutions has been studied by several methods. Over the years, interest has been shifted toward developing separation agents from a variety of low-cost agricultural byproducts as starting materials such as cellulosic materials (*1*), chitosan (*2*), tannin materials (*3,4*), etc. for precious metals

separation. The main advantages of using biomass wastes as adsorbents are an unlimited supply of feed materials, no production of secondary compounds such as sludge, biodegradability, and an environmentally friendly nature.

PGMs are can be present in the form of chloro-complexes. These forms are having very complicated solution chemistry. The species composition is dependent on factors such as chloride concentration, pH, ionic strength, temperature, and the age of the solution. The formation of metal complexes by PGMs is related to the solution composition. This in turn may affect the adsorption mechanism involved, i.e. chelation rather than ion exchange, and the affinity of the metal species for sorption sites on the adsorbents. Solution chemistry of PGMs is generally very different to that of base metals (*5*). When comparing to other PGMs, rhodium ions adsorption acidity is most strong one. This is another difficulty for adsorbents, they can be easily decompose or dissolve. In order to avoid this situation, synthesized biopolymer must have good acid resistance.

In our previous paper (*3*), we reported how successfully synthesize and characterize insoluble tannin polymer particles, however adsorption isotherm, thermodynamic and elution experiments has not performed. In this work, the adsorption behavior of valonea tannin resol polymer (TAR) particle toward Rh (III) ions in model solutions in strongly acidic conditions was investigated batchwise. For this purpose, the effects of particle size and dose of sawdust, pH, contact time and initial Rh (III) concentration were investigated. The Langmuir, Freundlich, Temkin, Dubinin–Radushkevich (D-R), and Redlich-Peterson (R-P) isotherms were used to fit the equilibrium data. This paper also presents the thermodynamic parameters such as Gibbs free energy change (ΔG°), enthalpy change (ΔH°) and entropy change (ΔS°) have been calculated and discussed. Langmuir and R-P constants of experimental data were calculated with nonlinear regression method using Microsoft Excel's Solver Extension software program. Chi-square test was used to evaluate the models which have best fit with experimental data. In addition, different stripping solutions were also investigated for elution of adsorbed Rh (III) ion from TAR particle surface.

2. Results and Discussion

2.1. Effect of pH

The pH of the aqueous solution is one of the important controlling parameter in the sorption process of PGMs. The effect of initial pH was studied at the pH ranges of 0-5 in 0.5 steps and results are shown in Figure 1. The amounts of adsorbed Rh (III) have been increased from 49.9 to 15.6 mg/g, with decrease in pH from 11 to 2.

Figure 1. Influence of pH on Rh (III) adsorption (C_{oTAR} =49.9 mg/L, 0.2 g TAR, 2930ºC, pCl=3, V=50 mL, t=60 min.)

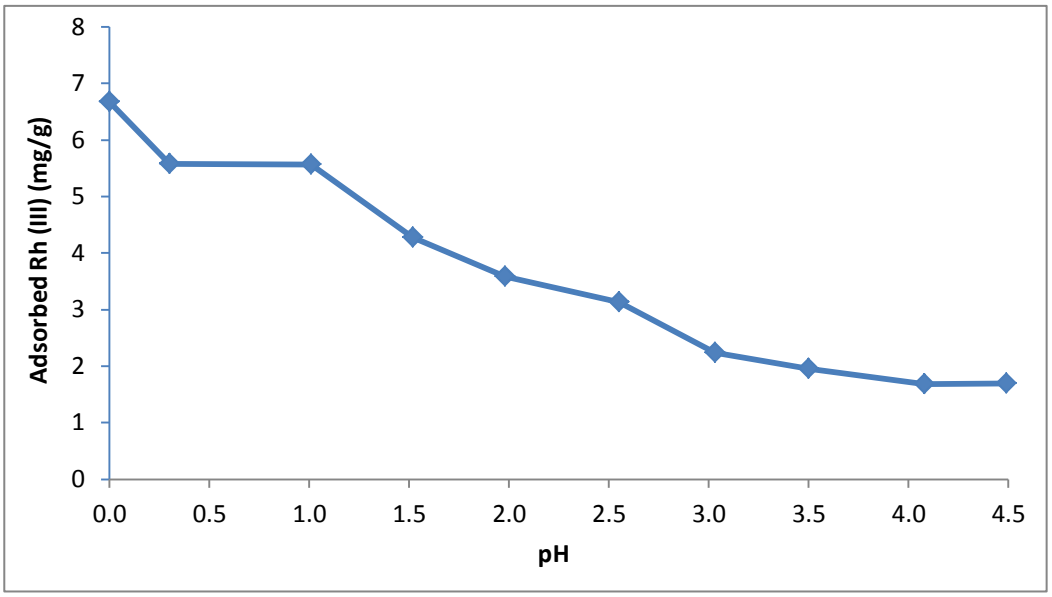

The adsorption capacity increases significantly with a decrease in the pH. The maximum dye removals were observed at pH 0. At this pH value, some part of TAR particle surface must be charged positively. In strong acid concentrations, a large amount of H_3O^+ was firstly or competitively adsorbed in the π sites (*6,7*). It is clear that when Rh (III) species are positively or natural charged, adsorption capacity will increase. To this end, the most suitable strategy is reducing [Cl^-] concentration. Thus from $Rh\ (H_2O)_6^{3+}$ to $RhCl_3(H_2O)_3^0$ species can be more adsorbed onto TAR surface at lower pH conditions.

2.2. Effect of the Cl^- concentration

In order to understand the effect of Cl^- concentration to adsorption of Rh (III) onto TAR particles, experiments were carried out in batch systems with different stirring rates changing from 10^{-3} – 1 M Cl^-. Obtained results are shown in Figure 2. As can be seen, adsorption capacity is higher at lower Cl^- concentration. This shows color ions having inhibitory effect to Rh (III) adsorption. In this conditions (1M [H+] and 10^{-3} M [Cl^-]), Rh (III) species which is from $Rh\ (H_2O)_6^{3+}$ to $RhCl_3(H_2O)_3^0$ are expected to be formed more than negatively charged Rh (III) species (from $RhCl_4(H_2O)_2^-$ to $RhCl_6^{3-}$). It can be observed that the increase in [Cl^-] leads to a decrease in Rh (III) adsorption capacities, from 17.42 mg g^{-1} to 13.25 mg g^{-1}. 10^{-3} M [Cl^-] has been selected for further subsequent experiments.

Figure 2. Influence of Cl^- concentration on Rh (III) adsorption (C_{oTAR} =49.9 mg/L, 0.2 g TAR, 2930ºC, pH=0, V=50 mL, t=60 min.)

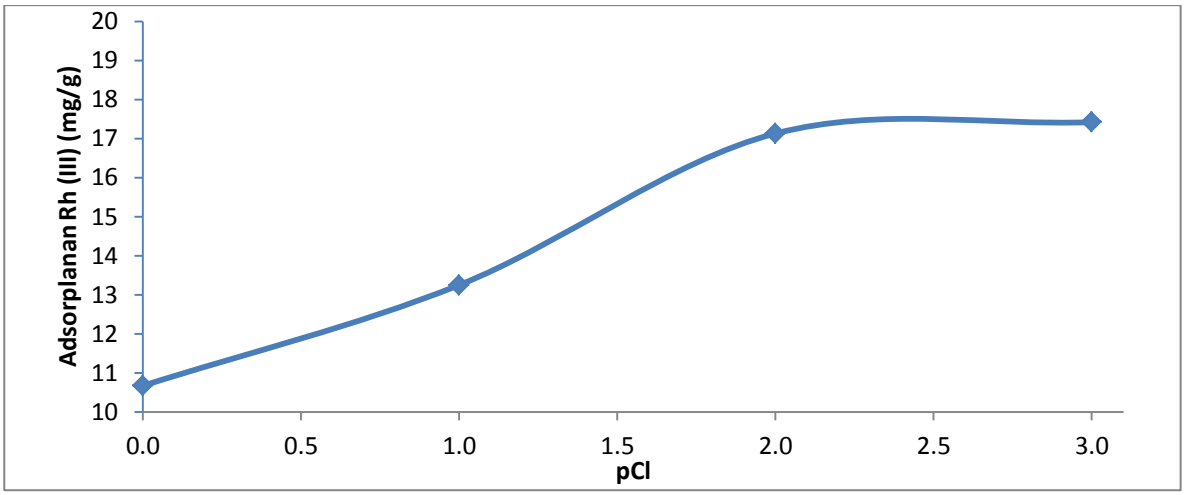

2.3. Effect of TAR mass

The effect of the adsorbent dosage on adsorptions of Rh (III) on TAR particle surface is shown in Figure 3. TAR mass was varied out between 0.025 – 0.15 g with 0.025 g steps and equilibrated for 60 min. It can be revealed from Figure 3 that the adsorption increases with increase in TAR mass. The efficiency was 4.894% at the adsorbent concentration of 0.5 g/L, while it is varied from 4.894% to 22.19% at adsorbent concentrations of 0.5–3 g/L for Rh (III), respectively. Although 5 times increase in adsorbent dosage, the removal greater than 0.5 g/L increased up to about 400 percent. Increasing the TAR dose the amount of adsorbed Rh (III) increases but adsorption density, adsorption density, decreases. This is due to the number of available adsorption sites increases by increasing the adsorbent dose. In addition, aggregation of particles may have a reductive impact to adsorption density. This situation will reduce surface area of adsorbents and increase diffusion path length. Thus, the equilibrium concentration is considered to be 0.1 g for TAR particles.

Figure 3. The effects of adsorbent dosage on RH (III) adsorption (pH_{TAR}=0, pCl_{TAR} = 3, C_{oTAR}=61,3 mg/L, 293ºK, V=50 mL, t=60 min.).

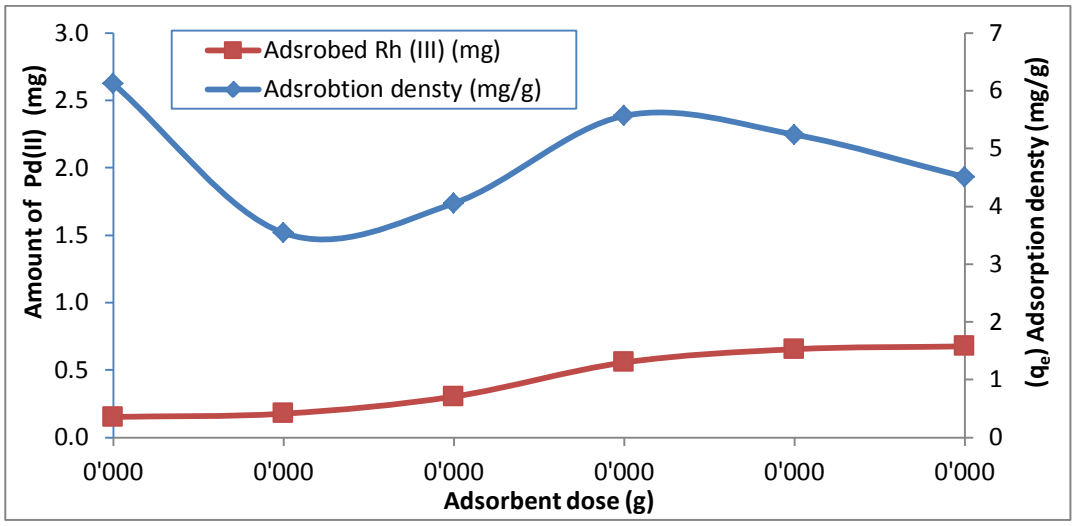

2.4. Effect of contact time and initial Rh (III) concentration

The preliminary experiments showed that the adsorption of Rh (III) is fast at the initial stages and becomes slower near the equilibrium. Figure 4 presents the plots of Rh (III) removal versus contact time for TAR particles at initial concentrations between 16.54 and 88.80 mg/L at 298 °K with a contact time of 150 min. The rate of dye removals are very rapid until 20 minute and plot flattens thereafter. It is revealed that there was no considerable change for adsorption of Rh (III) after 90 min. for varied initial concentrations. The equilibrium times are independent of initial Rh (III) concentration. With the increase in the initial Rh (III) concentration, the efficiency increases. This phenomenon can be explained by the high adsorption capacity of the TAR particles.

Figure 4. The effects of contact time and initial Rh (III) concentration on adsorption (pH=0, pC =3, 293ºK, V=1000 mL).

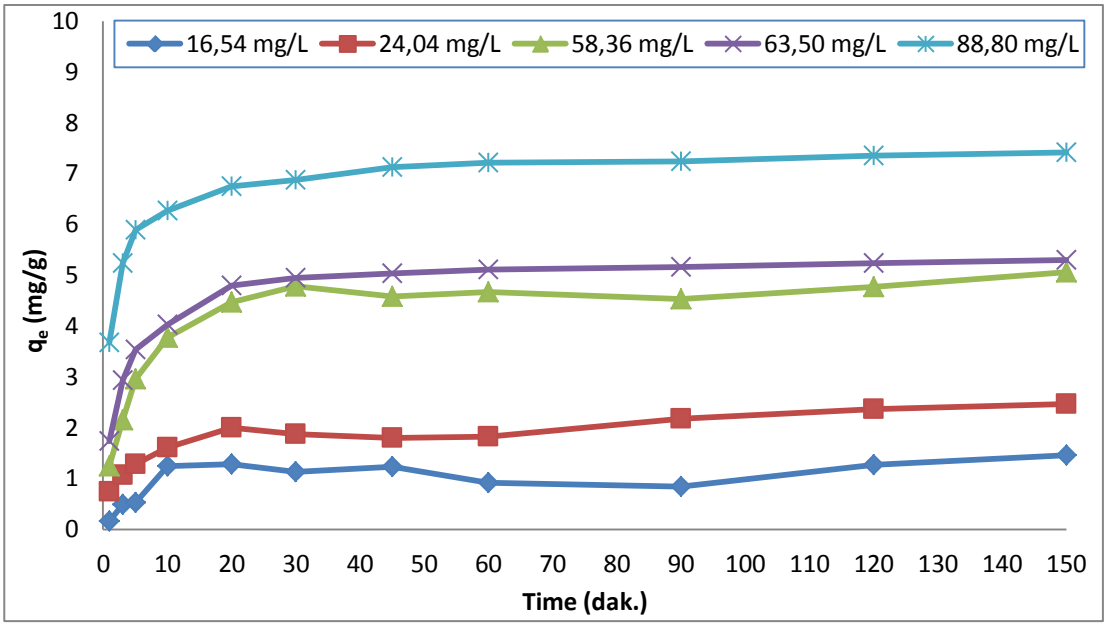

2.5. Adsorption isotherms

Four most using isotherms are selected in this study, which are, namely the Langmuir, Freundlich, Tempkin, Dubinin–Radushkevich, and Redlich-Peterson isotherms. A comparison of two linear and a nonlinear solve of Langmuir isotherm firstly carried out. Then, Freundlich, Tempkin, Dubinin–Radushkevich, and Redlich-Peterson, have been applied to the experiment of Rh (III) sorption on TAR particles. Here, at linear forms Pearson's correlation coefficient (r^2) error function and at nonlinear solutions Pearson's Chi-square (x^2) error function were taken into consideration and then for others, error function calculated. In addition to, in the nonlinear Langmuir solution, where the predicted values generated from a model different than linear regression, an r^2 value can be calculated between the measured q_e and modeled q_e data values. In this case, the value is not directly a measure of how good the modeled values are, but rather a measure of how good a predictor might be constructed from the modeled values. This usage is specifically the definition of the term "coefficient of determination": the square of the correlation between two variables.

Linear regression has been one of the most acceptable tool defining the best-fitting relationship quantifying the distribution of adsorbates, mathematically analyzing the adsorption systems and verifying the consistency and theoretical assumptions of an isotherm model. Contrary to the linearization models, nonlinear regression usually involves the minimization or maximization of error distribution (between the experimental data and the predicted isotherm) based on its convergence criteria. However, there is an opinion about nonlinear regression being also not statistically correct. This opinion is based on experimental errors in both the dependent and the independent variables in the isotherm equations (*8*). In this case, r^2 values for both linear forms of Langmuir isotherm were significantly different as summarized in Table 1. When just using the linear forms of Langmuir isotherms for comparison, Lineweaver-Burk linear form was suitable then Langmuir linear form for the experimental data. In contrary to this, when considering x^2 values, linear form of Langmuir was most suitable among the linearized two forms. Even though the most suitable isotherm for the dataset was Lineweaver-Burk form, the differences between the two linear forms of Langmuir isotherms have significantly in agreement with experimental results. Each linear equation has different axial settings individually so that would alter the result of a linear regression and influence the determination process. For this reason, it is not appropriate to use r^2 of linear regression analysis for comparing the best-fitting of Freundlich, Tempkin, Dubinin–Radushkevich, and both linear Langmuir isotherms. x^2 (Pearson's Chi-square) error function analysis could be a better method.

Table 1. Langmuir isotherm constants for Rh (III) adsorption onto TAR particles.

Isotherm	$\mathbf{K_L}$ (L/g)	$\mathbf{a_L}$ (L/mg)	$\mathbf{Q_{max}}$ (mg/g)	$\mathbf{R_L}$	r^2	x^2
Lineweaver-Burk linear	0.0985	0.0010	97,51	0.918 – 0.984	0.9999	0.0134
Langmuir linear	0.0987	0.0011	91.82	0.913 – 0.983	0.8050	0.0133
Nonlinear regression	0.0984	0.0010	96.69	0.917 – 0.983	0.9989	0.0134
Freundlich	$\mathbf{K_f}$ (L/g)	**n**			r^2	x^2
	9.230	1.040			0.9995	0.015
Tempkin	**A** (L/g)	**B** (j/mol)			r^2	x^2
	0.90	3.404			0.9600	0.171
Dubinin–Radushkevich	**β** $(mmol/j)^2$	$\mathbf{q_m}$ (mmol/g)	**E** (kJ/mol)		r^2	x^2
	0.639	5.962	0.885		0.8820	0.242
Redlich-Peterson	**K** (L/g)	**a** (L/mg)	**β**		r^2*	x^2
	0.0779	0.0031	0.9942		0.9909	0.037

Chi-square distribution value the Dubinin–Radushkevich and Tempkin isotherm was significantly higher than each value for Rh (III) dye adsorption onto red pine sawdust. Based on the x^2 values, as indicated in Table 1, nonlinear method is the best reliable method for solution of the Langmuir isotherm, can be said. Beyond that, the best fitting isotherm of the five studied isotherms are

Redlich-Peterson isotherm for Rh (III) adsorption. x^2 statistical tests were not able to reveal most appropriate between Redlich–Peterson and Langmuir model nonlinear approaches (in Table 1). Coefficient of determination (r^2) was able to point out the Langmuir nonlinear method as the most appropriate one (having r^2 0.9996 value). The facts, Due to Redlich-Peterson isotherm's β value is equal to 0.9942, hence the best reliable Langmuir isotherm solution is nonlinear regression this values can be considered. These confirm the monolayer coverage onto TAR surfaces and also the homogeneous distribution of active sites on the adsorbent, since the Langmuir equation assumes that the surface is homogeneous. According to Langmuir nonlinear method, monolayer saturation capacity of Rh (III) onto TAR particles was determined as 96.69 mg/g.

The calculated R_L values as different initial dye concentrations are shown in Figure 5. Dimensionless constant, R_L, indicates the shape of the isotherms to be either unfavorable ($R_L > 1$), linear ($R_L = 1$), favorable ($0 < R_L < 1$) or irreversible ($R_L = 0$). It is observed that, R_L values were determined between 0.917 – 0.983 for Rh (III) ions. This indicated that adsorptions were more favorable for the higher initial dye concentrations than for the lower ones. Langmuir isotherm constants, r^2, and x^2 values are listed in Table 1. Freundlich isotherm is widely applied in heterogeneous systems especially for organic compounds or highly interactive species on activated carbon and molecular sieves. The slope (1/n) ranges between 0 and 1 is a measure of adsorption intensity or surface heterogeneity, and it becomes more homogeneous when its value gets closer to one. Slopes of Rh (III) was determined as 0.9615. These results are further evidence of the surface homogeneity. Tempkin isotherm showing less agreement to the experimental data, x^2 values 0.171 for Rh (III), hence, it can be considered as indication of surface not heterogeneous. Here because of initial concentrations having relatively high (Table 1 Langmuir's R_L values), caused relatively low x^2 values for adsorption systems.

Figure 5. Plots of separation factor versus initial Rh (III) initial concentrations .

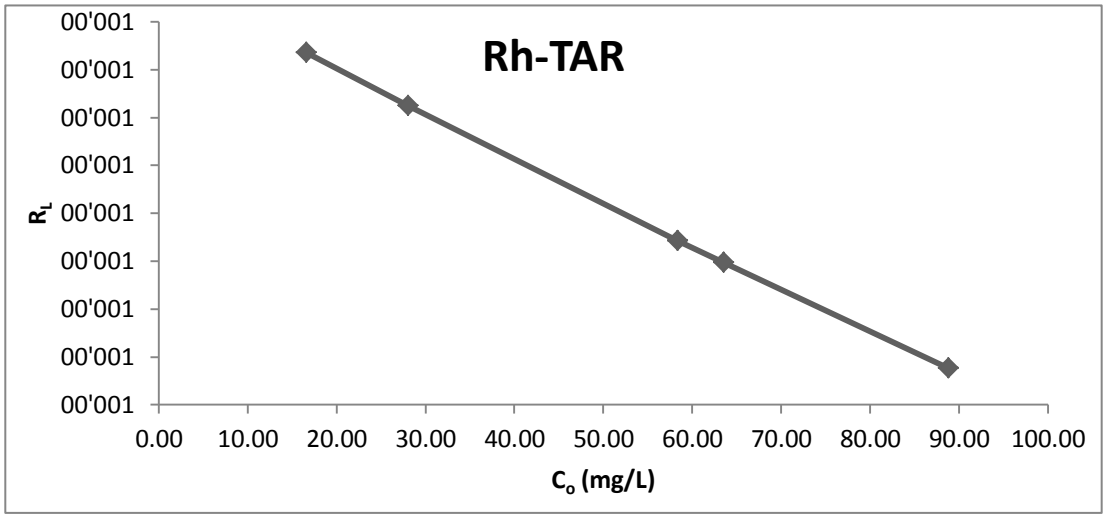

Dubinin-Radushkevich isotherm constant, β ($mmol^2/J^2$), has been used to the mean free energy (E) of sorption per mole of the adsorbate. E value calculated as 0.885 for Rh (III). Because of E is range of $8 < E < 16\ kJ/mol$, adsorption is governed by ion exchange mechanism (*9,10*). Using Langmuir's Q_{max} (mg/g) and Dubinin–Radushkevich's q_m (mmol/g) values, unknown molecular weight

of Rh (III) can be calculated approximately. The reason is, especially the Dubinin-Radushkevich isotherm, the compliance of isotherms to experimental data in low. The Redlich-Peterson isotherm parameters $K(\mathrm{L/g})$, $a(\mathrm{L/mg^{1-1/A}})$, $and\ \beta$ can be seen in Table 1. Because of isotherm unitless constant β values having 0.9942 for Rh (III), adsorption isotherm fits Langmuir isotherm. A comparison is also made between the experimental data and worked isotherms plotted in Figure 6. As can be seen from Table 1, the Langmuir, Freundlich, and Redlich-Peterson isotherms equations were show enough compliance to the experimental results. Despite of Dubinin-Radushkevich isotherm represents adsorption systems at low concentrations, Tempkin isotherm generally in more agreement experimental data than Dubinin-Radushkevich isotherm. Based on Figure 6, it can be say that the Redlich-Peterson isotherm was generates a satisfactory fit to the experimental data in all data points.

Figure 6. The measured and non-linear modeled time profiles for adsorption of the Rh (III) onto TAR particles (pH=0, pC =3, 293ºK, V=1000 mL).

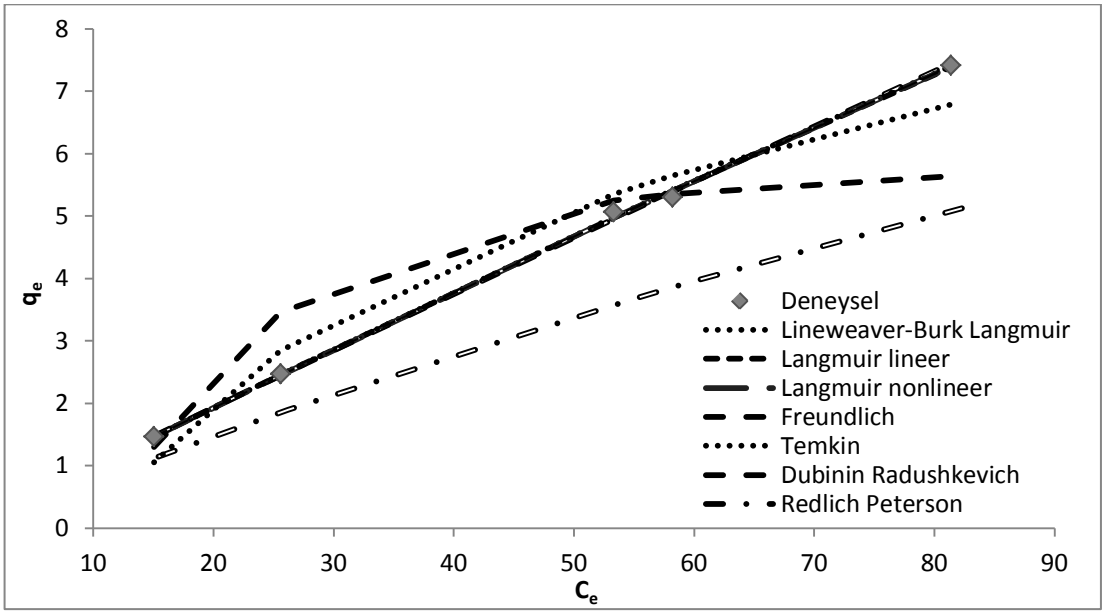

2.6. Effect of temperature on adsorption

In order to understand the effect of temperature on adsorption of Rh (III) ions TAR particles, herein, experiments at 293, 303, 313, 323, 333 and 343 °K temperatures were studied, and the results were shown in Figure 7. Results indicate that each amount adsorbed of Rh (III) ions decreases with an increase in temperature For example, for initial Rh (III) concentration of 67.1 mg/L (in 50 mL volumes), when increasing initial solution temperature from 298 to 353 °K, the amount of Rh (III) ions adsorbed per unit weight of TAR decreases 3.32 to 0.53 mg/g. The decrease in the adsorption capacity at increased temperature indicated the exothermic nature of the adsorption process of Rh (III) onto TAR.

Figure 7. Effect of temperature at the adsorption of Rh (III) ions.

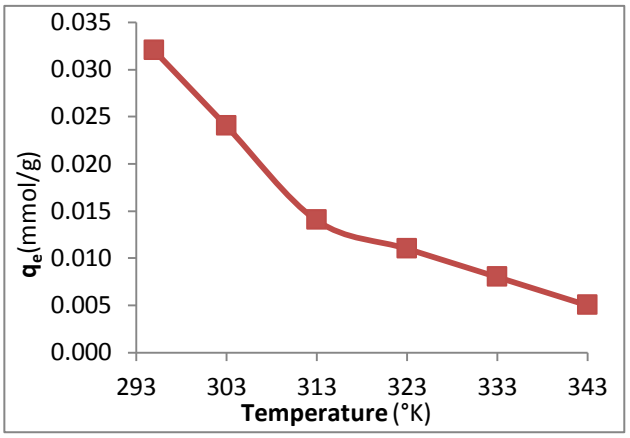

2.7.Determination of thermodynamic parameters

The plot of lnK_L against 1/T (in Kelvin) should be linear from which ΔH^o and ΔS^o were calculated from the slope and intercept, respectively. The slope of the van't Hoff plot is equal to $-\Delta H^0/R$, and its interception is equal to $\Delta S^0/R$ from equation *(10)*. The van't Hoff plot for the adsorption of Rh (III) onto TAR particles is given in Figure 7. Thermodynamic parameters obtained are given in Table 2. As shown in the table, the negative values of ΔG^0 at different temperatures indicate the spontaneous nature of the adsorption process.

Figure 8. van't Hoff graphic of the Rh (III) – TAR adsorption system.

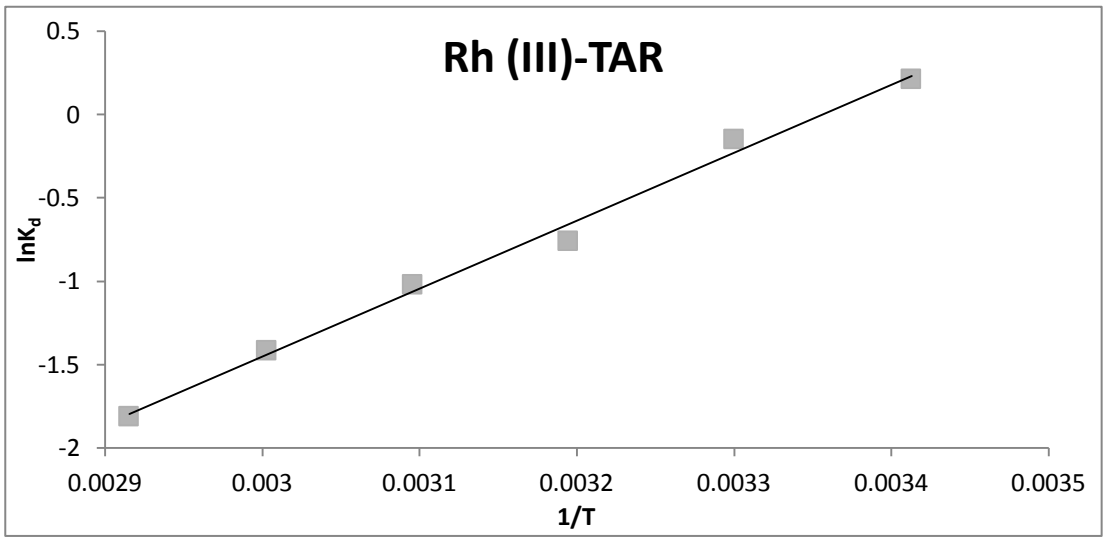

Table 2. Thermodynamic parameters for the adsorption of Rh (III) ions onto TAR particles.

ΔH^o (kJ/mol.K)	ΔS^o (J/mol.K)	ΔG^o (kJ/mol.K)			
		298 °K	313 °K	333 °K	353 °K
-33.87	-113.65	-0.513	0.372	1.981	2.736

The negative value of ΔH^o suggests the exothermic nature of adsorption system. Generally when ΔH^0 value if it smaller than 40 kJ/(mol.K), this interaction assumed as weak interaction or physisorption (*11*). Based on this study ΔH^0 values determined as -33.87 kJ/(mol.K) for Rh (III), and this suggested that the adsorption of Rh (III) ions onto TAR particles were physisorption process. The negative value of ΔS^0 suggests the decreased randomness at the solid/solution interface during the adsorption. As is well known, all systems move toward minimum energy and maximum randomness. Here, although randomness has decreased, the tendencies of systems toward minimum energy seem to be the dominant.

2.1. Desorption of Rh (III) ions

Desorption of Rh (III) ions from TAR particle surface was rapid and equilibrium was achieved within 1 h. The adsorption experiments were performed at optimum conditions and then recovery experiments were conducted. As shown in Table 3, different elation solution selected and most efficient one tried to determine. 38.86 percentage of adsorbed Rh (III) onto TAR particles desorbed with 1 M HNO_3 and 0.1 M $NaClO_3$ mixture. The low recovery values of all eluents may be attributed to the formation of stable complexes with TAR.

Table 3. The recovery efficiency of Rh (III) ions with different eluent.

Stripping solution	Recovery (%)
1 M HNO_3 + 0,1 M $NaClO_3$	38,86
1 M HNO_3 + 0,1 M NaClO	19,32
1 M HNO_3 + 0,1 M H_20_2	22,74

3. Experimental Section

3.1. Materials

Commercial valonea tannin extracts were obtained from Tuzla Dericiler Sanayi Sitesi, İstanbul-Türkiye. The extract, which is considered their tannin content, was used in the polymerization experiments without further purification. $RhCl_3.3H_2O$, NH_3, HCOH, HNO_3, HCl, NaCl and, NaOH purchased from Merck Company. AAS standard solutions for determination of PGM purchased form UltraScientific Company. All other reagents were analytical grade. The aqueous Rh (III) stock solution was prepared from solid $RhCl_3.3H_2O$ in 1.0 M HCl. The studied solutions of Rh (III) were obtained by dilution with NaOH or HNO_3 to adjust the H^+ concentration to the desired value. Moreover, a suitable chloride concentration was obtained. Preparation of TAR polymer was explained in detail at our recent publication dealing synthesis and characterization of polymer (*3*).

3.2. Adsorption Studies

The rhodium (III) solution was prepared by diluting stock solutions containing 200 mg/dm^3 metal ion in distilled water to 50 mg/L concentrations. 50 mL of metal ion solutions prepared for adsorption experiments and stirred after adding 200 mg TAR particles. The stirring rate was the same for all. All adsorption experiments were carried out in a standard and strictly adhered to batchwise system. Only adsorption capacity experiments were carried out by agitating 1g TAR with 1000 ml of metal solution of the various initial metal concentrations for 150 min (the time required for equilibrium to be reached between metal ions adsorbed and metal ions in solution). The experiments were performed at 300 rpm. The initial pH of the solutions controlled by adding a small amount of HCl, HNO_3, NaOH and $HClO_4$. At the end of the adsorption period, 15 mL samples were centrifuged and the solutions were filtered through a 0.45 μm Milipore filter paper to avoid any solid particle in the aqueous phase. Samples were measured using AAS. All the adsorption tests were performed at least twice so as to avoid wrong interpretation owing to any experimental errors. FAAS calibrated using 0, 4, 12 and 20 ppm standard solution for Rh (III) in 1M HCl. Samples diluted to measurement limits for precise results. Amount of adsorbed metal ions was calculated from the concentrations in solutions before and after adsorption process. Results were taken from the average of three scans for each sample.

3.3. Adsorption Isotherms

To simulate the adsorption isotherm, here five commonly used models, the Langmuir, Freundlich, Temkin, Dubinin–Radushkevich, and Redlich-Peterson, were selected to explicate metal ion–TAR interactions. These isotherms and its linear forms can be seen at Table 4.

The Langmuir equation initially derived from kinetic studies has been based on the assumption that on the adsorbent surface there is a definite and energetically equivalent number of adsorption sites. The bonding to the adsorption sites can be either chemical or physical, but it must be sufficiently strong to prevent displacement of adsorbed molecules along the surface. Thus, localised adsorption was assumed as being distinct from non-localised adsorption, where the adsorbed molecules can move along the surface. Because the bulk phase is constituted by a perfect gas, lateral interactions among the adsorbate molecules were neglected. On the energetically homogeneous surface of the adsorbent a monolayer surface phase is thus formed. Langmuir, for the first time, introduced a clear concept of the monomolecular adsorption on energetically homogeneous surfaces (*12*,*13*).

Although there have been five different linear form of Langmiur isotherm equation named as Langmuir (*12*), Competitive Langmuir (*14*), Lineweaver-Burk (*15*), Eadie-Hofstee (*16*,*17*,*18*), Scatchard (*19*), and log-log (*20*), two most commonly used form, given in Table 1. Lineweaver-Burk linear form (*15*), is very sensitive to errors, especially at the lower left corner of the chart, it is a very good agreement with to the experimental data (*20*,*21*). The K_L and a_L are the Langmuir isotherm constants and the K_L/a_L gives the theoretical monolayer saturation capacity, Q_0.

Table 4. Adsorption isotherms and its lineer forms.

	Isotherm	Linear Form	X & Y	Slope & cut-off point
Langmuir linear [12,13]	$q_e = \frac{K_L C_e}{1 + a_L C_e}$	$\frac{C_e}{q_e} = \frac{1}{K_L} + \frac{a_L C_e}{K_L}$	$x = C_e$ $y = C_e/q_e$	$\tan\alpha = \frac{a_L}{K_L}$ $cutoff = \frac{1}{K_L}$
Lineweaver-Burk linear [15]		$\frac{1}{q_e} = \frac{1}{K_L}\frac{1}{C_e} + \frac{a_L}{K_L}$	$x = 1/C_e$ $y = 1/q_e$	$\tan\alpha = \frac{1}{K_L}$ $cutoff = \frac{a_L}{K_L}$
Freundlich [22]	$q_e = K_f C_e^{1/n}$	$\log q_e = -\log K_f + \frac{1}{n}\log C_e$	$x = \log c_e$ $y = \log q_e$	$\tan\alpha = \frac{1}{n}$ $cutoff = -\log K_f$
Temkin [23]	$q_e = \frac{RT}{b}\ln(AC_e)$, $RT/b = B$	$q_e = B\ln A + B\ln C_e$	$x = \ln C_e$ $y = q_e$	$\tan\alpha = B$ $cutoff = B\ln A$
(D-R) [24,25]	$q_e = q_m e^{-\beta\varepsilon^2}$ $\varepsilon = RT\left(1 + \frac{1}{C_e}\right)$	$\ln q_e = \ln q_m - \beta\varepsilon^2$	$x = \varepsilon^2$ $y = \ln q_e$	$\tan\alpha = \beta$ $cutoff = q_m$
(R-P) [26]	$q_e = \frac{AC_e}{1 + BC_e^g}$	$\ln\left(A\frac{C_e}{q_e} - 1\right) = g\ln(C_e) + \ln(B)$	-	-

The essential features of the Langmuir isotherm can be expressed in terms of a dimensionless constant called separation factor (R_L) which is defined by the following equation

$$R_L = \frac{1}{1 + a_L C_o} \quad (1)$$

where C_0 (mg/L) is the initial dye concentration and a_L (L/mg) is the Langmuir constant related to the energy of adsorption. In this context, the value of R_L indicates the shape of the isotherms to be either unfavorable ($R_L > 1$), linear ($R_L = 1$), favorable ($0 < R_L < 1$) or irreversible ($R_L = 0$) (*27*,*28*).

Freundlich isotherm is widely applied in heterogeneous systems especially for organic compounds or highly interactive species on activated carbon and clays. The Freundlich isotherm is an empirical equation employed to describe heterogeneous systems and equation shown in Table 1. In this equation,K_f, ($mg^{1-1/n}L^{1/n}g^{-1}$) is the Freundlich constant related to the bonding energy, and n, (g/L) is the heterogeneity factor. The slope (1/n) ranges between 0 and 1 is a measure of adsorption intensity or surface heterogeneity, and it becomes more heterogeneous when its value gets closer to zero. Whereas, a value below unity implies chemisorptions process where 1/n above one is an indicative of cooperative adsorption (*27*,*29*).

This model is the earliest known relationship describing the non-ideal reversible multilayer adsorption with non-uniform distribution of adsorption heat and affinities over the heterogeneous surface. In this perspective, the amount adsorbed is the summation of adsorption on all sites (each having bond energy), with the stronger binding sites are occupied first, until adsorption energy are exponentially decreased upon the completion of adsorption process (*30*). Its linearized and non-linearized equations are listed in Table 1. Freundlich isotherm is criticized for its limitation of lacking a fundamental thermodynamic basis, not approaching the Henry's law at vanishing concentrations (*31*).

By ignoring the extremely low and large value of concentrations, the derivation of the Temkin isotherm assumes that the fall in the heat of sorption is linear rather than logarithmic. Temkin equation is excellent for predicting the gas phase equilibrium, conversely complex adsorption systems including the liquid-phase adsorption isotherms are usually not appropriate to be represented (*32*). In this equation, A (L/mg) is the equilibrium binding constant corresponding to the maximum binding energy, b (J/mol) is Temkin isotherm constant and constant B (dimensionless) is related to the heat of adsorption.

Radushkevich (*25*) and Dubinin (*24*) have reported that the characteristic sorption curve is related to the porous structure of the sorbent (Table 1). Where the constant, β, ($mmol^2/J^2$) is D-R constant related to the mean free energy of sorption per mole of the sorbate as it is transferred to the surface of the solid from infinite distance in the solution and can be correlated using fallowing relationship

$$E = \frac{1}{\sqrt{2\beta}} \qquad (2)$$

and q_m, (mmol/g) is denoted as the single layer capacity. In a deeper explanation, E value indicates the mechanism of the adsorption reaction. When $E < 8\ kJ/mol$, physical forces may affect the adsorption. If E is $8 < E < 16\ kJ/mol$, adsorption is governed by ion exchange mechanism, while for the values of $E > 18\ kJ/mol$, adsorption may be dominated by particle diffusion (*9*). The model has often successfully fitted high solute activities and the intermediate range of concentrations data well, but has unsatisfactory asymptotic properties and does not predict the Henry's law at low pressure (*27*). Meanwhile, the parameter ε known as Polanyi potential and can be correlated as

$$\varepsilon = RT\left(1 + \frac{1}{C_e}\right) \qquad (3)$$

where R, T and C_e represent the gas constant (8.314 J/mol K), absolute temperature (K) and adsorbate equilibrium concentration (mg/L), respectively.

The Redlich-Peterson isotherm contains three parameters ($A(\mathrm{L/g}), B(\mathrm{L/mg^{1-1/A}}), g$) and incorporates the features of the Langmuir and the Freundlich isotherms [(26)]. Its equation and linear form can be seen in Table 1. Isotherm unitless constants g is gives between $0 < g < 1$ values. When$g = 1$, adsorption isotherm fits Langmuir isotherm. If $g = 0$, isotherm is now fully Freundlich isotherm (*27*,*33*). Values between this concerned for isotherm representation. Due to having this versatility, it can be applied either in homogeneous or heterogeneous systems.

Hence, because of containing tree constant, it has been presented that the non-linear method is a better way to obtain the isotherm parameters. A trial-and-error procedure, which is applicable to computer operation, was used to compare the best fit of the three isotherms using an optimization routine to minimize the coefficient of determination sum of the squares of the errors, between the experimental data and isotherms in the solver add-in with Microsoft's Excel (*34*). In addition, the Redlich-Peterson isotherm equation can be resolved to the linear regression method by making it linear form.

3.4.Error Analysis

Linear regression has been one of the most viable tools defining the best-fitting relationship quantifying the distribution of adsorbates, mathematically analyzing the adsorption systems and verifying the consistency and theoretical assumptions of an isotherm model (*27*). Concomitant with the development of computer technology, the progression of the nonlinear isotherm modeling has extensively been facilitated. Contrary to the linearization models, nonlinear regression usually involves the minimization or maximization of error distribution between the experimental data and the predicted isotherm based on its convergence criteria (*33*). In this study two error functions, the coefficient of determination and nonlinear chi-square test have been used for analyzing the adsorption system.

Coefficient of determination, which represents the percentage of variability in the dependent variable (the variance about the mean) is employed to analyze the fitting degree of isotherm and kinetic models with the experimental data (*27*). Coefficient of determination is defined as (*35*)

$$r^2 = \frac{\sum(q_{e,meas}-\overline{q_{e,calc}})^2}{\sum(q_{e,meas}-\overline{q_{e,calc}})^2+(q_{e,meas}-q_{e,calc})^2} \quad (4)$$

where $q_{e,meas}$ (mg/g) is the amount of dye exchanged by the surface of red pine sawdust obtained from experiment, $q_{e,calc}$ the amount of dye obtained by isotherm models and $\overline{q_{e,calc}}$ the average of $q_{e,calc}$ (mg/g). Its value may vary from 0 to 1, and the higher the r^2 values, means the model is more useful. Essentially, r^2 tells us how much better we can do in predicting $q_{e,meas}$ by using the model and computing $q_{e,calc}$ than by just using the mean $\overline{q_{e,calc}}$ as a predictor.

Nonlinear chi-square test is a statistical tool necessary for the best fit of an adsorption system, obtained by judging the sum squares differences between the experimental and the calculated data, with each squared difference is divided by its corresponding value (calculated from the models). Small χ^2 value indicates its similarities while a larger number represents the variation of the experimental data (*27*,*34*).

$$X^2 = \sum_{i=1}^{n} \frac{(q_{e,calc}-q_{e,meas})^2}{q_{e,meas}} \quad (5)$$

4. Adsorption Thermodynamic

Thermodynamic parameters such as Gibb's free energy (ΔG^0), enthalpy change (ΔH^0) and change in entropy (ΔS^0) for the adsorption of dye on red pine sawdust have been determined by using the following equations

$$\Delta G^0 = \Delta H^0 - T\Delta S^0 \quad (6)$$

$$\Delta G^0 = -RT\ln(K_L) \quad (7)$$

$$K_L = \frac{q_e}{C_e} \quad (8)$$

$$\log(\frac{q_e}{C_e}) = \frac{\Delta S^0}{2.303\ R} - \frac{\Delta H^0}{2.303\ RT} \quad (9)$$

where q_e is the amount of dye adsorbed per unit mass of pine cone (mg/g), C_e is equilibrium concentration (mg/L) and T is temperature in K and R is the gas constant (8.314 J/molK). Considering the relationship between ΔG^0 and K_L, ΔH^0 and ΔS^0 were determined from the slope and intercept of the van't Hoff plots of log(K_L) versus 1/T. Negative values of ΔG^0 confirm the feasibility of the process and the spontaneous nature of the adsorption [36,37,38]. In general, the ΔH^0 value of physisorption is smaller than 40 kJ/mol (*36*). The positive value of ΔH^0 is indicating that the adsorption reaction was endothermic (*39*,*36*,*40*). The negative entropy change ($\Delta S°$) for the process was caused by the decrease in degree of freedom of the adsorbed species (*41*).

4. Conclusions

The adsorption of Rh (III) ions has been studied with TAR resin particles. The acidity solutions and the adsorption temperature were effective in the adsorption of Rh (III) ions. It was found that TAR had Rh (III) monolayer adsorption capacity (q_m) of 96.69 mg Rh (III)/g TAR. Here, the adsorption data fitted better to the Langmuir isotherm then other four isotherms. The Gibbs free energies ($\Delta G°$) were calculated changing from −0.513 kJ/mol to 2.735 kJ/mol at 293 °K to 343 °K, respectively. These $\Delta G°$ values show that a spontaneous adsorption process occurs at room temperature. The enthalpy change ($\Delta H°$), and the entropy change ($\Delta S°$) were -33.87 kJ/mol and -113.65 J/mol, respectively. Adsorbed Rh (III) ions can be desorbed mixture of 1 M HNO_3 and 0.1 M $NaClO_3$ solutions with 38.86% efficiency.

Acknowledgment

This work is supported by the Scientific Research Project Commission (BAPK) of Sakarya University (Project No: 2014-34-10-001).

Conflicts of Interest

The authors declare no conflict of interest.

References and Notes

1. Goto, M.; Kasaini, H.; Furusaki, S. Selective Separation of Pd(II), Rh(III), and Ru(III) Ions from a Mixed Chloride Solution Using Activated Carbon Pellets. *Seperation Science and Technology* **2000,** *35*, 1307–1327.
2. Alam, M. S.; Inoue, K.; Yoshizuka, K.; Ishibashi, H. Adsorptive Separation of Rhodium(lll) Using Fe(Ill)-Templated Oxine Type of Chemically Modified Chitosan. *Separation Science and Technology* **1998,** *33* (5), 655-666.
3. Can, M.; Bulut, E.; Örnek, A.; Özacar, M. Synthesis and characterization of valonea tannin resin

and its interaction with palladium (II), rhodium (III) chloro complexes. *Chemical Engineering Journal* **2013,** *221,* 146–158.

4. Can, M.; Bulut, E.; Özacar, M. Synthesis and characterization of pyrogallol-formaldehyde nano resin and its usage as adsorbent. *Journal of Chemical & Engineering Data* **2012,** *57* (10), 2710–2717.
5. Godlewska-Zylkiewicz, B. Biosorption of platinum and palladium for their separation/preconcentration prior to graphite furnace atomic absorption spectrometric determination. *Spectrochimica Acta* **2003,** *58,* 1531–1540.
6. Ullmann's Encyclopedia of Industrial Chemistry,Hesse, Wolfgang. *Phenolic Resins;* Wiley VCH: Wiesbaden. Germany, 2004.
7. Can, M. Vibrational Spectroscopy of Pyrogallol with a glance on the problems of formation of a dimer. *Research Journal of Chemistry and Environment* **2013,** *17* (12), 117-128.
8. El-Khaiary, M. I. Least-squares regression of adsorption equilibrium data: Comparing the options. *Journal of Hazardous Materials* **2008,** *158,* 73–87.
9. Özcan, A. S.; Erdem, B.; Özcan, A. Adsorption of Acid Blue 193 from aqueous solutions onto BTMA-bentonite. *Colloids and Surfaces A: Physicochemical and Engineering Aspects* **2005,** *266* (1-3), 73-81.
10. Can, M. Equilibrium, kinetics and process design of acid yellow 132 adsorption onto red pine. *Journal of Environmental Management* **2014**.
11. Wataru, S.; Yoshinobu, K. . Method of preparing insoluble hydrolysable tannin and method of treating waste liquid with the tannin. 0527096A2, 1992.
12. Langmuir, I. The Adsorption Of Gases On Plane Surface Of Glass, Mica And Platinum. *Journal of the American Chemical Society* **1918,** *40,* 1361–1403.
13. Langmuir, I. The constitution and fundamental properties of solids and liquids. *Journal Of The American Chemical Society* **1916,** *38,* 2221–2295.
14. Altın, O.; Özbelge, H. Ö.; Doğu, T. Use of General Purpose Adsorption Isotherms for Heavy Metal–Clay Mineral Interactions. *Journal of Colloid and Interface Science* **1998,** *198,* 130-140.
15. Lineweaver, H.; Burk, D. The Determination of Enzyme Dissociation Constants. *Journal of the American Chemical Society* **1934,** *56,* 658–666.
16. Eadie, G. S. The inhibition of cholinesterase by physostigmine and prostigmine. *Journal Of Biological Chemistry* **1942,** 85-93.
17. Eadie, G. S. On the Evaluation of the Constants Vm and KM in Enzyme Reactions. *Science* **1952,** 688.
18. Hofstee, B. H. J. On the evaluation of the constants Vm and KM in enzyme reactions. *Science* **1952,** 329-331.
19. Scatchard, G. The attractions of proteins for small molecules and ions. *Annals Of The New York Academy Of Science* **1949,** *51,* 660-672.
20. El-Khaiary, M. I. Least-squares regression of adsorption equilibrium data: Comparing the options.

Journal of Hazardous Materials **2008,** *158,* 73–87.

21. Bolster, C. H.; Hornberger, G. M. On the Use of Linearized Langmuir Equations. *Soil Science Society of America Journal* **2007,** *71,* 1796-1806.
22. Freundlich, H. M. F. Über die adsorption in lösungen. *Z. Phys. Chem.* **1906,** *57,* 385–471.
23. Temkin, M. I. Adsorption Equilibrium and Kinetics of Processes on Heterogeneous Surfaces and at Interaction between Adsorbed Molecules. *Zh. Fiz. Khim.(Russian Journal Of Physical Chemistry)* **1941,** *15,* 296.
24. Dubinin, M. M. Modern state of the theory of volume filling of micropore adsorbents during adsorption of gases and steams on carbon adsorbents. *Zhurnal Fizicheskoi Khimii* **1965,** *39,* 1305–1317.
25. Radushkevich, L. V. Potential theory of sorption and structure of carbons. *Zhurnal Fizicheskoi Khimii* **1949,** *23,* 1410–1420.
26. Redlich, O.; Peterson, D. L. A Udeful Adsorpsiton Isotherm. *The Journal of Physical Chemistry A* **1959,** *63,* 1024.
27. Foo, K. Y.; Hameed, B. H. Insights into the modeling of adsorption isotherm systems. *Chemical Engineering Journal* **2010,** *156,* 2-10.
28. Webber, T. W.; Chakkravorti, R. K. Pore and solid diffusion models for fixed-bed adsorbers. *AlChE Journal* **1974,** *20,* 228–238.
29. Crini, G.; Peindy, H. N.; Gimbert, F.; Robert, C. Removal of C.I. Basic Green 4 (Malachite Green) from aqueous solutions by adsorption using cyclodextrin-based adsorbent: Kinetic and equilibrium studies. *Separation and Purification Technology* **2007,** *53,* 97-110.
30. Dabrowski, A. Adsorption - from theory to practice. *Advances in Colloid and Interface Science* **2001,** *93* (135-224), 135-224.
31. Ho, Y. S.; Porter, J. F.; McKay, G. Equilibrium isotherm studies for the sorption of divalent metal ions onto peat: Copper, nickel and lead single component systems. *Water, Air, and Soil Pollution* **2002,** *141* (1-4), 1-33.
32. Kim, Y.; Kim, C.; Choi, I.; Rengraj, S.; Yi, J. Arsenic Removal Using Mesoporous Alumina Prepared via a Templating Method. *Environmental Science & Technology* **2004,** *38* (3), 924-931.
33. Kumar, K. V.; Sivanesan, S. Comparison of linear and non-linear method in estimating the sorption isotherm parameters for safranin onto activated carbon. *Journal of Hazardous Materials* **2005,** *123,* 288-292.
34. Ho, Y. S. Selection of optimum sorption isotherm. *Carbon* **2004,** *42,* 2113–2130.
35. Ho, Y. S. Second-order kinetic model for the sorption of cadmium onto tree fern: a comparison of linear and non-linear methods. *Water Research* **2006,** *40* (1), 119–125.
36. Yao, Y.; Xu, F.; Chen, M.; Xu, Z.; Zhu, Z. Adsorption behavior of methylene blue on carbon nanotubes. *Bioresource Technology* **2010,** *101,* 3040–3046.
37. Hong, S.; Wen, C.; Hea, J.; Gana, F.; Ho, Y.-S. Adsorption thermodynamics of Methylene Blue onto bentonite. *Journal of Hazardous Materials* **2009,** *167,* 630–633.

38. Farooq, U.; Kozinski, J. A.; Khan, M. A.; Athar, M. Biosorption of heavy metal ions using wheat based biosorbents – A review. *Bioresource Technology* **2010,** *101,* 5043–5053.
39. Kara, M.; Yuzer, H.; Sabah, E.; Celik, M. S. Adsorption of cobalt from aqueous solutions onto sepiolite. *Water Research* **2003,** *37,* 224-232.
40. Liu, Y.; Liu, Y.-J. Biosorption isotherms, kinetics and thermodynamics. *Separation and Purification Technology* **2008,** *61,* 229–242.
41. Aydın, Y. A.; Aksoy, N. D. Adsorption of chromium on chitosan: Optimization, kinetics and thermodynamics. *Chemical Engineering Journal* **2009,** *151,* 188-194.